Generalized Minimal Principle for Rotor Filaments

Hans Dierckx,[1] Marcel Wellner,[2] Olivier Bernus,[3] and Henri Verschelde[1]
[1]Department of Mathematical Physics and Astronomy, Ghent University, 9000 Ghent, Belgium
[2]Physics Department, Syracuse University, Syracuse, New York 13244, USA
[3]L'Institut de Rythmologie et Modélisation Cardiaque, Université de Bordeaux, 33604 Pessac, France
(Received 29 August 2014; revised manuscript received 24 March 2015; published 30 April 2015)

To a reaction-diffusion medium with an inhomogeneous anisotropic diffusion tensor $\mathbf{D}$, we add a fourth spatial dimension such that the determinant of the diffusion tensor is constant in four dimensions. We propose a generalized minimal principle for rotor filaments, stating that the scroll wave filament strives to minimize its surface area in the higher-dimensional space. As a consequence, stationary scroll wave filaments in the original 3D medium are geodesic curves with respect to the metric tensor $\mathbf{G} = \det(\mathbf{D})\mathbf{D}^{-1}$. The theory is confirmed by numerical simulations for positive and negative filament tension and a model with a non-stationary spiral core. We conclude that filaments in cardiac tissue with positive tension preferentially reside or anchor in regions where cardiac cells are less interconnected, such as portions of the cardiac wall with a large number of cleavage planes.

DOI: 10.1103/PhysRevLett.114.178104 PACS numbers: 87.19.Hh, 87.10.-e, 05.45.-a

Introduction.—Phase singularity lines known as filaments are present in many natural systems [1–4]. Filaments are remarkably persistent features, since they are topologically protected and therefore must be closed or end on medium boundaries. They often act as organizing centers, as in the case of hydrodynamical [4] or superconducting [1] vortices, crystallographic defects [2], oscillating chemical reactions [3] and cardiac arrhythmias [5–8]. Being organizing centers, filaments tend to dominate the dynamics of the entire system if they are present, e.g., in hurricanes, type II superconductors, chemical oscillations and cardiac fibrillation [1,3,7,8]. Thus, studying the dynamics and stability of filaments will help to characterize and understand the entire system.

Despite their diverse nature, filaments in homogeneous media tend to behave geometrically. A useful characteristic is the total length of a filament: for a hydrodynamical vortex—a conservative system—filament length is preserved over time [4]. In contrast, in dissipative reaction-diffusion systems such as cardiac tissue, filament length changes monotonically [9]; its length decreases if the so-called filament tension γ_1 of the medium is positive [9]. In such a case, filament rings will shrink and vanish, while a "transmural" filament (i.e., connecting opposite medium boundaries) can only be in stable equilibrium if its length is minimal. Hence, for $\gamma_1 > 0$, the stationary filament shape in an isotropic parallel slab is a straight line.

However, some media exhibit anisotropic wave propagation, which complicates their mathematical description. An important example is cardiac tissue, which is anisotropic due to its fibrous structure. Moreover, steep spatial variations in fiber direction were found to destabilize transmural filaments [10] and form cusp waves [11]. Also, the equilibrium configuration of a filament was numerically found to be a trade-off between a straight line and following the local fiber direction [12,13]. This property was elegantly summarized by Wellner *et al.* [13], who showed analytically for a class of "deformed" anisotropy that a minimal principle holds: the stationary filaments are geodesic curves if one recognizes the anisotropic diffusion tensor as the inverse metric of the space considered. A more general proof for Wellner's minimal principle based on response functions and Fermi coordinates is presented in [14]. In the curved-space viewpoint [13–16], more accurate laws of motion for wave fronts [17] and spiral waves [18] have been derived for anisotropic reaction-diffusion systems.

A key assumption in the current proofs for the minimal principle is that the diffusion tensor's determinant $|\mathbf{D}|$ should be constant in time and space. However, gradients in $|\mathbf{D}|$ are known to cause filament drift (see, e.g., [15]), and may therefore change the stationary filament shape and position. To go beyond the condition of constant $|\mathbf{D}|$ is interesting in cardiac tissue applications, since laminar clefts decrease the diffusivity in portions of the ventricular wall [19,20], and transmural gradients in the expression of intercellular gap junctions [21] lead to inhomogeneous $|\mathbf{D}|$. Moreover, during cardiac ischemia, diffusion is reduced [22]. Although chemical systems are mostly modeled as isotropic, the diffusivity and therefore $|\mathbf{D}|$ may vary spatially in experiments.

In this Letter, we show that the modified metric $\mathbf{G} = \mathbf{D}^{-1}|\mathbf{D}|$ introduced in [23] for isotropic media gives rise to a generalized minimal principle that is also valid in anisotropic excitable media with varying determinant of the diffusion tensor. We rely on a geometric argument to show that this view does not necessarily conflict with calculations in the usual metric $\mathbf{g} = \mathbf{D}^{-1}$ [13]. Finally, we apply the generalized minimal principle. First, our results justify the equivalence between filament tension coefficients and metric

drift coefficients. Second, we reinterpret literature results on scroll wave drift from [23–25]. Third, numerical simulations confirm the theoretical prediction that filaments with positive tension will drift to the lowest diffusive coupling, while negative tension filaments drift towards higher diffusive coupling.

Methods.—We are interested in the properties of stationary scroll wave solutions to the reaction-diffusion (RD) equations

$$\partial_t \mathbf{u} = \partial_i (D^{ij} \partial_j \mathbf{P}\mathbf{u}) + \mathbf{F}(\mathbf{u}), \tag{1}$$

where $\mathbf{u}$ is the vector of state variables. In cardiac models, the constant matrix $\mathbf{P}$ ensures that only the first variable (transmembrane potential) can diffuse, while in models of chemical systems $\mathbf{P}$ is usually taken to be the identity matrix. It can be observed [14] that the anisotropic diffusion term in Eq. (1) is highly similar to a covariant Laplacian $\mathcal{D}^2$; the latter trivially transforms (i.e., is covariant) under a change of coordinates. For a general metric $\mathbf{h}$ with determinant $|\mathbf{h}|$, one has under a coordinate change $x^i \to x'^{i'}$ that

$$\mathcal{D}^2 f = \frac{\partial_i(\sqrt{|\mathbf{h}|} h^{ij} \partial_j f)}{\sqrt{|\mathbf{h}|}} = \frac{\partial_{i'}(\sqrt{|\mathbf{h}'|} h^{i'j'} \partial_{j'} f)}{\sqrt{|\mathbf{h}'|}}. \tag{2}$$

There are several ways to recognize the covariant Laplacian (2) in Eq. (1). First, if $|\mathbf{D}|$ is assumed constant in space, the correspondence is exact if one defines $g^{ij} = D^{ij}$ (see, e.g., [13,14,16,18,25,26]):

$$\mathbf{g} = (g_{ij}) = \mathbf{D}^{-1}, \qquad g := |\mathbf{g}| = |\mathbf{D}|^{-1}. \tag{3}$$

Second, one may equate the bracketed quantities in the diffusion term and covariant Laplacian to propose $\sqrt{G} G^{ij} = D^{ij}$, whence

$$\mathbf{G} = (G_{ij}) = \mathbf{D}^{-1} |\mathbf{D}|, \qquad G := |\mathbf{G}| = |\mathbf{D}|^2. \tag{4}$$

The latter formulas were first obtained by Wellner and co-workers [23,27], in an isotropic medium with linear diffusivity gradient. Filament statics in an isotropic medium with an abrupt change in diffusion coefficient are studied in [28].

There are several ways to prove that the metric (4) also describes filament statics in generic anisotropic media. In our variational derivation, a fourth spatial dimension is added, in which the scroll wave is invariant; we show that minimizing the filament's surface area in the 4D space is equivalent to finding geodesics of the 3D metric (4).

Let us now explicitly perform the geometric embedding of an anisotropic medium with inhomogeneous $|\mathbf{D}|$. For three-dimensional scroll waves, we imagine a fourth spatial dimension called w in which the rotating scroll wave solution is left invariant: $\mathbf{u}_4(x, y, z, w, t) = \mathbf{u}(x, y, z, t)$. This dimension may be assigned finite length W and periodic or no-flux boundary conditions. The diffusion coefficient in the additional direction is chosen to be $1/|\mathbf{D}| = |\mathbf{g}|$, with $\mathbf{g}$ the metric (3), which measures distances in terms of plane-wave arrival times [14,29]. In 4D Cartesian coordinates, we obtain the extended metric $\tilde{\mathbf{g}}$

$$\tilde{\mathbf{g}} = \begin{pmatrix} g_{xx} & g_{yy} & g_{zz} & 0 \\ g_{xy} & g_{yy} & g_{yz} & 0 \\ g_{xz} & g_{yz} & g_{zz} & 0 \\ 0 & 0 & 0 & |\mathbf{D}| \end{pmatrix}, \tag{5}$$

which does not depend on the new coordinate w. Moreover, it was constructed to possess determinant $|\tilde{\mathbf{g}}| = 1$. When embedding a scroll wave into four dimensions, the filament also extends in the w direction, so that it becomes a surface, which one may choose to call a "brane" or "worldsheet" as in string theory [30]. A filament with fixed end points now becomes a brane with fixed boundary lines parallel to the W axis.

Following the Fermi-coordinates approach used in Refs. [14,15], we can show that instead of minimizing its length, the two-dimensional filament brane will strive to minimize its surface area with respect to the metric $\tilde{\mathbf{g}}$. The detailed proof falls outside our present scope and will be presented elsewhere. Using such a higher-dimensional minimal principle, a stationary filament brane will minimize its surface area $S = \iint \sqrt{|\tilde{\mathbf{g}}|}\, dw ds$, given by the Nambu-Goto string action [30]:

$$\begin{aligned} S &= \iint dw \sqrt{\tilde{g}_{ww}} \sqrt{g_{ij} \frac{\partial x^i}{\partial s} \frac{\partial x^j}{\partial s}}\, ds \\ &= W \int \sqrt{(g_{ij}|\mathbf{D}|) \frac{\partial x^i}{\partial s} \frac{\partial x^j}{\partial s}}\, ds \\ &= W \int \sqrt{G_{ij} \frac{\partial x^i}{\partial s} \frac{\partial x^j}{\partial s}}\, ds. \end{aligned} \tag{6}$$

This short derivation shows that minimizing filament surface area with respect to $\tilde{\mathbf{g}}$ using the classical minimal principle boils down to minimize filament length with respect to $\mathbf{G} = \mathbf{g}|\mathbf{D}|$, according to Eq. (4).

Results.—We now provide several examples that illustrate the power of the generalized minimal principle. Let us first apply the embedding idea to the drift of a spiral wave on a two-dimensional surface with anisotropic diffusion and varying $|\mathbf{D}|$, as shown in Fig. 1(a). Extending the medium in the W direction with $D^{ww} = 1/|\mathbf{D}|$, one sees that in the resulting three-dimensional medium, the diffusion has constant determinant equal to one again. Here, we can use Wellner's original minimal principle [13] in three dimensions, to find that stationary filaments will reside at a site where they have extremal length. It is well known that in a medium where filaments have positive tension γ_1, their length will be minimized [9]. Thus, when $\gamma_1 > 0$, the filament of the embedded spiral wave will end up in a locus where $D^{ww} = 1/|\mathbf{D}|$ is maximal. On the contrary, in models where the reaction kinetics yield $\gamma_1 < 0$, the filament will drift to a region with minimal $D^{ww} = 1/|\mathbf{D}|$. In this case, a

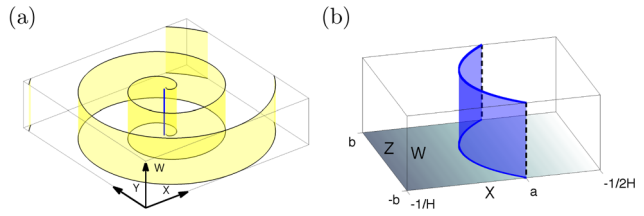

FIG. 1 (color online). Understanding stationary filament shapes by adding an additional dimension W. (a) By adding an extra dimension W to a spiral wave in the XY plane, the spiral's rotation center becomes a filament curve in XYW space. (b) Filament in an isotropic 3D space, pinned at both ends $(x, y, z) = (a, 0, \pm b)$ under a gradient H of the diffusion coefficient D [23]; the spatial Y dimension is not drawn here. By embedding, the filament curve is extended to a brane around which the scroll wave rotates in four dimensions. Dark shading indicates low D.

negative tension instability is not allowed to develop since the filament curve is defined to remain parallel to the W axis.

From recent work [18], it is known that in two dimensions, the Riemann curvature of the medium will also induce drift of spiral waves on a surface. However, if one works in the limit of slowly varying anisotropy compared to the spatial rate of change of $|\mathbf{D}|$, the drift induced by the gradient of $|\mathbf{D}|$ will prevail and determine the stationary filament positions. Furthermore, nonvanishing Riemann tensor components in the extended space (e.g., R_{xwxw}) cannot affect the filament dynamics, since all state variable fields are invariant in the w direction. Also, due to the block-diagonal structure of $\tilde{\mathbf{g}}$, Riemann tensor components along the original spatial directions (e.g., R_{xyxy}) remain unaffected by the embedding.

Note further that the intramural filaments in a rotational anisotropy setting as studied in [24,25] are essentially spiral waves in a medium with inhomogeneous diffusion. The reasoning above now predicts that intramural filaments will drift to a layer where they are parallel to the local fiber direction only when $\gamma_1 > 0$; for negative tension, they will end up perpendicular to the local fiber direction, confirming the discussion in [25].

As a second application, consider a three-dimensional scroll wave in the half plane $x > -1/H$, with scalar diffusivity $D^{ij} = (1 + Hx)\delta^{ij}$, where $H > 0$. It was shown in [23] that a filament pinned at $x = a$, $y = 0$, $z = \pm b$ takes the shape $x = -1/H + A\cosh(z/A)$ with A defined by $1 + aH = AH\cosh(b/A)$ to satisfy the pinning conditions. This solution was found to be a geodesic of $\mathbf{G}$ defined by Eq. (4). From the embedding viewpoint depicted in Fig. 1(b), we extend the medium in a fourth dimension w with $D^{ww} = (1 + Hx)^{-3}$ to note that the filament brane is pulled to the region of small x, since its surface area measure $dw/\sqrt{D^{ww}}$ in the fourth dimension is more favorable there. In general, if $\gamma_1 > 0$ we expect from the higher-dimensional minimal principle that stationary filaments will tend to reside in regions with small $|\mathbf{D}|$, i.e., in regions where the medium has the lowest diffusive coupling.

Geometry for numerical simulations.—Let us consider thirdly a relevant example from cardiac anatomy. Classically, the thick ventricular wall is modeled as consisting of local myofibers aligned in the direction $\vec{e}_f$, i.e.,

$$D^{ij}(\vec{r}) = D_s\delta^{ij} + (D_f - D_s)e_f^i(\vec{r})e_f^j(\vec{r}), \tag{7}$$

with $D_f \approx 3D_s$ [10,13]. The fibers are found to rotate through the myocardial wall over an angle close to 120° [31], with left-handed chirality. A widely used simplified model for cardiac anisotropy, known as rotational anisotropy [10,11,13,24], is given on the domain $(x, y, z) \in (0, L_x) \times (0, L_y) \times (0, L_z)$ by

$$\vec{e}_f(\vec{r}) = \cos\alpha(z)\vec{e}_x + \sin\alpha(z)\vec{e}_y. \tag{8}$$

The fiber helix angle α is often assumed to be linearly increasing with transmural coordinate z.

From histological [32] and high-resolution MRI studies [33], however, the cardiac myofibers in the midwall region were found to be organized in sheets, separated by cleavage planes that reduce mechanical shear stresses during contraction [19,20]. We shall here model the layered architecture of myocardial tissue by reducing diffusivity along the sheet normal direction in the central part of the myocardial wall in the direction normal to the cleavage plane orientation. As a result, the tissue is modeled as orthotropic. Instead of Eq. (7) we take [34]

$$D^{ij} = D_f e_f^i e_f^j + D_s e_s^i e_s^j + D_n e_n^i e_n^j, \tag{9}$$

where the main diffusivities $D_f > D_s \geq D_n > 0$ occur along the fiber $(\vec{e}_f)$, sheet $(\vec{e}_s)$, and sheet normal $(\vec{e}_n)$ direction, which are mutually orthogonal. Sheet presence is modeled using an orthotropy parameter $\eta(\vec{r}) \in [0, 1]$: $D_f = D_1$, $D_s = D_2$, $D_n = \eta D_2 + (1 - \eta)D_3$. Here, we set $D_1 = 5$, $D_2 = 1$, $D_3 = 0.33$ to match anisotropy ratios in pig ventricular tissue experiments [35]. For the myofiber and sheet normal directions, we take

$$\vec{e}_f(z) = \cos\alpha(z)\vec{e}_x + \sin\alpha(z)\vec{e}_y, \tag{10}$$

$$\vec{e}_n(z) = \sin\alpha(z)\vec{e}_x - \cos\alpha(z)\vec{e}_y, \tag{11}$$

with fiber helix angle $\alpha(z) = \pi/3 - 2\pi z/(3L_z)$. Since it is well known that sheets are absent in the subepicardium [19,20], we set $\eta = 0$ for $z > z_1 = 0.8L_z$. In our simulations, we assume the orthotropy parameter $\eta(x, z)$ piecewise linear in x, with $x_1 = 0.3L_x$, $x_2 = 0.7L_x$:

$$\eta(x,z) = \begin{cases} \eta_x(x) & 0 \leq z < z_1 \\ 0 & z_1 \leq z \leq L_z, \end{cases}$$

$$\eta_x(x) = \begin{cases} 0.5 + 0.5x/x_1 & 0 \leq x < x_1 \\ (x - x_1)/(L_x - x_1) & x_1 \leq x < x_2 \\ 1 - 0.5(x - x_2)/(L_x - x_2). & x_2 \leq x \leq L_x. \end{cases} \tag{12}$$

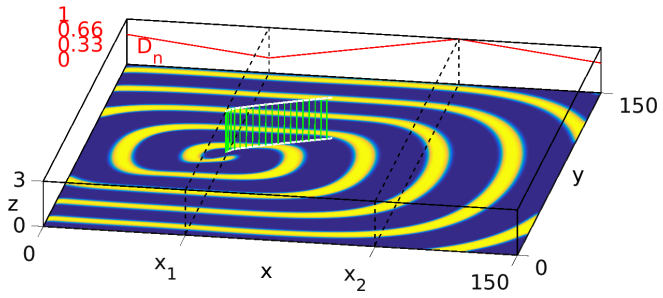

FIG. 2 (color online). Drift of a transmural filament (green) in a medium with rotational anisotropy and varying diffusivity $D_n(x,z)$. Filament rendered every 100 time units, and epi- and endocardial trajectory shown in white. Barkley's kinetics [36] were used with $a = 0.7$; bottom surface color denotes u at $t = 2000$.

For the geometry considered, the length of a straight transmural filament with respect to the metric $\mathbf{g}$ is $L_g = L_z/\sqrt{D_s}$ and therefore constant along the wall. Thus, from the original minimal principle, no drift is expected. However, according to the generalized minimal principle, the filament strives to minimize its length with respect to the metric $\mathbf{G}$, i.e., $L_G = (1-z_1)L_z\sqrt{D_1 D_3} + z_1 L_z\sqrt{D_1(D_2 - \eta(D_2 - D_3)}]$. Hence the filament will be stationary where η is extremal.

Numerical results.—Figures 2–3 show the drift trajectory for a filament with Barkley kinetics [36], i.e., $\mathbf{u} = [u, v]^T$, $\mathbf{F} = [(u/\epsilon)(1-u)(u-(v+b)/a, u-v]^T$ and $\mathbf{P} = \mathrm{diag}(5,0)$. We take domain size $L_x = 150$, $L_y = 150$, $L_z = 3$, lattice step $dx = 0.3$ and explicit Euler time step $dt = 0.0027$. We chose parameter values $b = 0.01$, $\epsilon = 0.025$ and $a = 0.7$ or $a = 0.4$ to cover the positive and negative filament tension regimes [37]. For $a = 0.7$, $\gamma_1 > 0$ and we see in the simulation that the filament is attracted to $x = x_1$, i.e., the zone with lowest diffusive coupling, as predicted by the generalized minimal principle. For $a = 0.4$ and $L_y = 225$, we have $\gamma_1 < 0$, but the wall is thin enough not to cause full 3D instability [17]. Instead, the original transmural (I) filament produces short-lived filaments (U) whose endpoints lie on the endocardial surface, where they appear as clockwise (CW) or counterclockwise (CCW) rotating spiral waves. Their trajectory is shown in Fig. 3. Note that despite this instability, the "mother" filament slowly drifts towards $x = x_2$, as predicted by the generalized minimal principle.

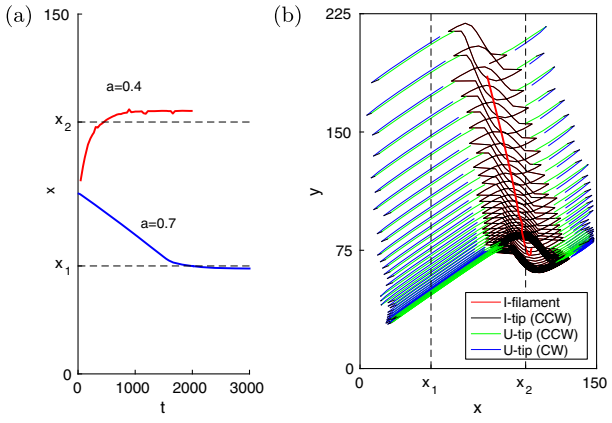

FIG. 3 (color online). (a) Epicardial drift trajectory for filaments in Barkley's model with positive ($a = 0.7$) and negative filament tension ($a = 0.4$). (b) Endocardial drift trajectories for the negative tension case ($a = 0.4$), in which case the original transmural (I) filament pinches off secondary U-shaped filaments at the endocardial side. The generalized minimal principle predicts filament attraction to $x = x_2$ (black, dashed). See movie in the Supplemental Material [38].

Second, we performed a numerical simulation with the minimal model for epicardial cells as proposed in [39]. We used grid resolution $dx = dy = 0.6$ and $dz = 0.4$ mm and domain size $L_x = 360$ mm, $L_y = 180$ mm, $L_z = 2.4$ mm, diffusion coefficient $\hat{\mathbf{P}} = \mathrm{diag}(0.1171, 0, 0)$ mm^2/ms [39], orthotropy ratio as above and time step 0.092 ms. Although this model has a linear core, Fig. 4 shows that its filament is attracted to the plane $x = x_1$ with the most pronounced laminar structure, as predicted by the generalized minimal principle in the case of positive filament tension.

Discussion.—In this Letter, we have generalized the minimal principle for scroll wave filaments to anisotropic media with inhomogeneous diffusivity. We presented a variational derivation due to its simplicity and the additional geometrical insights it offers. E.g., the direction of drift easily follows from the sign of filament tension and the filament length (surface) after embedding.

We also recall that the standard and generalized minimal principle for filaments are lowest order descriptions in curvature, twist, and anisotropy compared to the scroll wave core size [14]. In Figs. 2–3, two manifestations of higher order dynamics can be noted. First, the equilibrium position is not exactly x_1 or x_2, due to the different slopes of $D_n(x)$, which are felt by the finite-size scroll wave core. Second, since the medium is translationally invariant in Y, the minimal principle does not prefer one particular y value, and higher order corrections make the final filament state slowly drift in the Y direction.

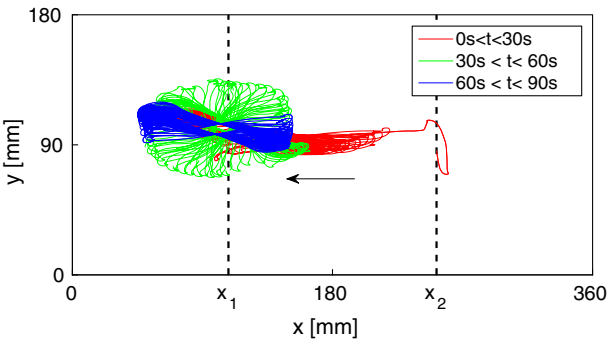

FIG. 4 (color online). Tip trajectory of a scroll wave in the minimal cardiac model by Bueno-Orovio, Cherry, and Fenton [39] in a slab geometry with fiber rotation and varying cleavage plane density. Every 1 s, the tip trajectory on the epicardial surface is shown during 0.3 s; the arrow indicates drift direction.

We further note that in thin tissue such as the atrial wall, filaments will remain straight and transmural due to their rigidity [17], even in the case of negative filament tension. Thus, given a cardiac geometry, one could measure the effective wall thickness with respect to metric **G** to find the filament attractors. Note that this result will be largely independent of the physiological reaction kinetics since they do not affect **D** or **G**; the effect of tension becoming negative is that repulsive loci will become attractive and vice versa. In principle, our method can thus be used to identify stable loci in the cardiac wall where rotors preferentially reside. Such application may be promising, as novel ablation strategies targeting rotors are currently being developed [8,40].

We are grateful to Arkady Pertsov and Ivan Kazbanov for helpful discussions. H. D. thanks the FWO-Flanders for funding. Simulations were performed at the HPC Centre of Ghent University.

[1] A. A. Abrikosov, On the magnetic properties of superconductors of the second group, Sov. Phys. JETP **5**, 1174 (1957).

[2] R. W. Siegel, in *Point Defects and Defect Interactions in Metals*, edited by J.-I. Takamura (North Holland, Amsterdam, 1981), P. 783.

[3] W. Jahnke, W. E. Skaggs, and A. T. Winfree, Chemical vortex dynamics in the Belousov-Zhabotinskii reaction and in the two-variable oregonator model, J. Phys. Chem. **93**, 740 (1989).

[4] R. L. Ricca, Physical interpretation of certain invariants for vortex filament motion under LIA, Phys. Fluids A **4**, 938 (1992).

[5] W. Baxter, S. F. Mironov, A. V. Zaitsev, A. M. Pertsov, and J. Jalife, Visualizing excitation waves in cardiac muscle using transillumination, Biophys. J. **80**, 516 (2001).

[6] A. M. Pertsov, in *Computer Simulation and Experimental Assessment of Cardiac Electrophysiology*, edited by N. Virag, O. Blanc, and L. Kappenberger (Futura, Lausanne, 2001), pp. 63–68.

[7] R. H. Clayton, E. A. Zhuchkova, and A. V. Panfilov, Phase singularities and filaments: Simplifying complexity in computational models of ventricular fibrillation, Prog. Biophys. Molec. Biol. **90**, 378 (2006).

[8] M. Haissaguerre *et al.*, Driver domains in persistent atrial fibrillation, Circulation **130**, 530 (2014).

[9] V. N. Biktashev, A. V. Holden, and H. Zhang, Tension of organizing filaments of scroll waves, Phil. Trans. R. Soc. A **347**, 611 (1994).

[10] F. H. Fenton and A. Karma, Vortex dynamics in three-dimensional continuous myocardium with fiber rotation: filament instability and fibrillation, Chaos **8**, 20 (1998).

[11] O. Bernus, M. Wellner, and A. M. Pertsov, Intramural wave propagation in cardiac tissue: asymptotic solutions and cusp waves, Phys. Rev. E **70**, 061913 (2004).

[12] O. Berenfeld, M. Wellner, J. Jalife, and A. M. Pertsov, Shaping of a scroll wave filament by cardiac fibers, Phys. Rev. E **63**, 061901 (2001).

[13] M. Wellner, O. M. Berenfeld, J. Jalife, and A. M. Pertsov, Minimal principle for rotor filaments, Proc. Natl. Acad. Sci. U.S.A. **99**, 8015 (2002).

[14] H. Verschelde, H. Dierckx, and O. Bernus, Covariant Stringlike Dynamics of Scroll Wave Filaments in Anisotropic Cardiac Tissue, Phys. Rev. Lett. **99**, 168104 (2007).

[15] H. Dierckx, O. Bernus, and H. Verschelde, A geometric theory for scroll wave filaments in anisotropic excitable tissue, Physica (Amsterdam) **238D**, 941 (2009).

[16] R. J. Young and A. V. Panfilov, Anisotropy of wave propagation in the heart can be modeled by a Riemannian electrophysiological metric, Proc. Natl. Acad. Sci. U.S.A. **107**, 15063 (2010).

[17] H. Dierckx, O. Selsil, H. Verschelde, and V. N. Biktashev, Buckling of Scroll Waves, Phys. Rev. Lett. **109**, 174102 (2012).

[18] H. Dierckx, E. Brisard, H. Verschelde, and A. V. Panfilov, Drift laws for spiral waves on curved anisotropic surfaces, Phys. Rev. E **88**, 012908 (2013).

[19] I. J. LeGrice, B. H. Smaill, L. Z. Chai, S. G. Edgar, J. B. Gavin, and P. J. Hunter, Laminar structure of the heart: ventricular myocyte arrangement and connective tissue architecture in the dog, Am. J. Physiol. **269**, H571 (1995).

[20] S. H. Gilbert, A. P. Benson, P. Li, and A. V. Holden, Regional localisation of left ventricular sheet architecture: integration with current models of cardiac fibre, sheet and band structure, Eur J Cardio Thorac Surg Suppl **32**, 231 (2007).

[21] S. Poelzing and D. S. Rosenbaum, Altered connexin43 expression produces arrhythmia substrate in heart failure, Am. J. Physiol.: Heart Circ. Physiol. **287**, H1762 (2004).

[22] A. G. Kléber, C. B. Riegger, and M. J. Janse, Electrical uncoupling and increase of extracellular resistance after induction of ischemia in isolated, arterially perfused rabbit papillary muscle, Circ. Res. **61**, 271 (1987).

[23] M. Wellner, C. Zemlin, and A. M. Pertsov, Frustrated drift of an anchored scroll-wave filament and the geodesic principle, Phys. Rev. E **82**, 036122 (2010).

[24] O. Berenfeld and A. M. Pertsov, Dynamics of intramural scroll waves in a 3-dimensional continuous myocardium with rotational anisotropy, J. Theor. Biol. **199**, 383 (1999).

[25] M. Wellner, O. Berenfeld, and A. M. Pertsov, Predicting filament drift in twisted anisotropy, Phys. Rev. E **61**, 1845 (2000).

[26] H. Dierckx, O. Bernus, and H. Verschelde, Accurate Eikonal-Curvature Relation for Wave Fronts in Locally Anisotropic Reaction-Diffusion Systems, Phys. Rev. Lett. **107**, 108101 (2011).

[27] M. Wellner, Rotation of a scroll wave reveals the metric tensor for the associated geodesic filament, Phys. Rev. E **91**, 032903 (2015).

[28] C. W. Zemlin, F. Varghese, M. Wellner, and A. M. Pertsov, Refraction of Scroll-Wave Filaments at the Boundary Between Two Reaction-Diffusion Media, Phys. Rev. Lett. **114**, 118303 (2015).

[29] K. H. W. ten Tusscher and A. V. Panfilov, Eikonal Formulation of the Minimal Principle for Scroll Wave Filaments, Phys. Rev. Lett. **93**, 108106 (2004).

[30] B. Zwiebach, *A First Course in String Theory* (Cambridge University Press, Cambridge, England, 2004).

[31] D. D. Jr. Streeter, Gross morphology and fiber geometry of the heart, in *Handbook of Physiology.-Section 2: The Cardiovascular System, Volume I: The Heart* (Am. Physiol. Soc., Bethesda, MD, 1979), p. 61.

[32] D. A. Hooks, M. L. Trew, B. J. Caldwell, G. B. Sands, I. J. LeGrice, and B. H. Smaill, Laminar arrangement of ventricular myocytes influences electrical behavior of the heart, Circ. Res. **101**, e103 (2007).

[33] S. H. Gilbert, D. Benoist, A. P. Benson, E. White, S. F. Tanner, A. V. Holden, H. Dobrzynski, O. Bernus, and A. Radjenovic, Visualization and quantification of whole rat heart laminar structure using high-spatial resolution contrast-enhanced MRI, Am. J. Physiol. **302**, H287 (2012).

[34] R. H. Clayton, O. Bernus, E. M. Cherry, H. Dierckx, F. H. Fenton, L. Mirabella, A. V. Panfilov, F. Sachse, G. Seemann, and H. Zhang, Models of cardiac tissue electrophysiology: Progress, challenges and open questions, Prog. Biophys. Molec. Biol. **104**, 22 (2011).

[35] B. J. Caldwell, M. L. Trew, G. B. Sands, D. A. Hooks, I. J. LeGrice, and B. H. Smaill, Three distinct directions of intramural activation reveal nonuniform side-to-side electrical coupling of ventricular myocytes, Circ Arrhythm Electrophysiol **2**, 433 (2009).

[36] D. Barkley, A model for fast computer simulation of waves in excitable media, Physica (Amsterdam) **49D**, 61 (1991).

[37] V. Hakim and H. Henry, Scroll waves in isotropic excitable media: linear instabilities, bifurcations and restabilized states, Phys. Rev. E **65**, 046235 (2002).

[38] See Supplemental Material at http://link.aps.org/supplemental/10.1103/PhysRevLett.114.178104 for a movie of the filament drift and break-up described in Fig. 3.

[39] A. Bueno-Orovio, E. M. Cherry, and F. H. Fenton, Minimal model for human ventricular action potentials in tissue, J. Theor. Biol. **253**, 544 (2008).

[40] S. M. Narayan, D. E. Krummen, K. Shivkumar, P. Clopton, W.-J. Rappel, and J. M. Miller, Treatment of atrial fibrillation by the ablation of localized sources, J. Am. Coll. Cardiol. **60**, 628 (2012).